1-2017

Effect of Fe substitution on the structural, magnetic and electron-transport properties of half-metallic Co2TiSi

Y. Yin
University of Nebraska - Lincoln

J. Waybright
South Dakota State University

See next page for additional authors

Effect of Fe substitution on the structural, magnetic and electron-transport properties of half-metallic Co_2TiSi

Y. Jin,[1,2] J. Waybright,[2,3] P. Kharel,[2,3] I. Tutic,[4] J. Herran,[5] P. Lukashev,[4] S. Valloppilly,[2] and D. J. Sellmyer[1,2]
[1]*Department of Physics and Astronomy, University of Nebraska, Lincoln, Nebraska 68588, USA*
[2]*Nebraska Center for Materials and Nanoscience, University of Nebraska, Lincoln, Nebraska 68588, USA*
[3]*Department of Physics, South Dakota State University, Brookings, South Dakota 57007, USA*
[4]*Department of Physics, University of Northern Iowa, Cedar Falls, Iowa 50614, USA*
[5]*Department of Chemistry and Biochemistry, University of Northern Iowa, Cedar Falls, Iowa 50614, USA*

(Presented 1 November 2016; received 19 September 2016; accepted 27 October 2016; published online 11 January 2017)

The structural, magnetic and electron-transport properties of $Co_2Ti_{1-x}Fe_xSi$ (x = 0, 0.25, 0.5) ribbons prepared by arc-melting and melt-spinning were investigated. The rapidly quenched $Co_2Ti_{0.5}Fe_{0.5}Si$ crystallized in the cubic $L2_1$ structure whereas $Co_2Ti_{0.75}Fe_{0.25}Si$ and Co_2TiFe_0Si showed various degrees of B2-type disorder. At room temperature, all the samples are ferromagnetic, and the Curie temperature increased from 360 K for Co_2TiSi to about 800 K for $Co_2Ti_{0.5}Fe_{0.5}Si$. The measured magnetization also increased due to partial substitution of Fe for Ti atoms. The ribbons are moderately conducting and show positive temperature coefficient of resistivity with the room temperature resistivity being between 360 μΩcm and 440 μΩcm. The experimentally observed structural and magnetic properties are consistent with the results of first-principle calculations. Our calculations also indicate that the $Co_2Ti_{1-x}Fe_xSi$ compound remains nearly half-metallic for x ≤ 0.5. The predicted large band gaps and high Curie temperatures much above room temperature make these materials promising for room temperature spintronic and magnetic applications. [http://dx.doi.org/10.1063/1.4974281]

I. INTRODUCTION

Magnetic materials including half-metallic ferro-, ferri-, and antiferromagnets that conduct electrons of only one spin channel have recently attracted a lot of attention due to their potential for spintronic devices.[1–6] Half-metals with the metallic electronic band structure for one spin channel and an insulating band structure for the opposite spin channel are of special interest because they are expected to produce an electron current of only one spin orientation i.e., show nearly 100% transport spin-polarization. Recent theoretical and experimental investigations have indicated that some Co-based Heusler alloys including Co_2MnSi, Co_2FeSi, Co_2FeAl have shown half-metallic band properties with high Curie temperature much above room temperature, making them potential candidates for room temperature spintronic applications.[7–10] One of the issues with these materials is the difficulty of synthesizing them in completely ordered $L2_1$ structures. Most experimentally reported compounds are either partially B2-type or A2-type disordered. Certain types of structural disorder are detrimental to half-metallic properties.[11] Further, for the robustness of half-metallic properties the materials need to have large band gap. These considerations stimulated this work where we aimed to synthesize Co_2TiSi, which has been predicted to be half metallic with large band gap of 0.621 eV,

with high degree of structural order.[7,12] Since the Curie temperature of Co_2TiSi is close to room temperature, we replaced certain fraction of Ti with Fe to increase its Curie temperature. Experimentally, we investigated three samples with compositions $Co_2Ti_{1-x}Fe_xSi$ (x = 0, 0.25, 0.5). Prior report shows that a partial Fe substitution for Cr in Co_2CrAl substantially increases its Curie temperature.[13] In this paper, we present our experimental results on the structural, magnetic and electron-transport properties of $Co_2Ti_{1-x}Fe_xSi$ (x = 0, 0.25, 0.5) compounds and compare the experimentally observed data with the results of our first-principle calculations.

II. METHODS

A. Experimental methods

Ingots of $Co_2Ti_{1-x}Fe_xSi$ (x = 0, 0.25, 0.5) compounds were prepared by arc melting high-purity elements in an argon atmosphere. The ribbon samples, which are about 2 mm wide and 50 μm thick, were made by rapid quenching in a melt spinner where induction-melted pieces of the ingots were ejected from a quartz tube onto the surface of a copper wheel rotating with a speed of 25 m/s. The crystal structures of the samples were investigated using powder x-ray diffraction (XRD) in Rigaku Miniflex and PANalytical Empyrean diffractometers with copper Kα radiation. Magnetic properties and electron-transport properties were investigated with a Quantum Design VersaLab magnetometer and Physical Properties Measurement system (PPMS). The elemental compositions of the films were determined using the energy-dispersive X-ray spectroscopy (EDX) in FEI Nova NanoSEM450. In all magnetic measurements, the external magnetic field was applied parallel to the length of the ribbon.

B. Computational methods

We performed density functional calculations of electronic and magnetic structures of Heusler compounds, $Co_{16}Ti_{(8-x)}Fe_xSi_8$, using the projector augmented-wave method (PAW),[14] implemented in the Vienna *ab initio* simulation package (VASP)[15] within the generalized-gradient approximation (GGA).[16] The integration method[17] with a 0.05 eV width of smearing is used, along with the plane-wave cut-off energy of 500 eV and convergence criteria of 10^{-2} meV for atomic relaxation, and 10^{-3} meV for the total energy and electronic structure calculations. A *k*-point mesh of 12 × 12 × 12 is used for the Brillouin-zone integration. 16-atom cubic cell is used, with periodic boundary condition imposed. For all ground state calculations, unit cell geometry was fully optimized to obtain equilibrium structures. Some of the results are obtained using the MedeA® software package.[18]

III. RESULTS AND DISCUSSION

A. Experimental results

Figure 1(a) shows the x-ray diffraction (XRD) patterns of $Co_2Ti_{1-x}Fe_xSi$ (x = 0, 0.25, 0.5) powder prepared from corresponding ribbon samples. The patterns of Co_2TiSi and $Co_2Ti_{0.5}Fe_{0.5}Si$ contain both the fundamental and the (111) and (002) superlattice peaks indicating that the samples mainly have cubic Heusler $L2_1$ structure. However, the absence of (111) peak in the pattern of $Co_2Ti_{0.75}Fe_{0.25}Si$ suggests that the sample contain strong B2-type disorder. In order to find the degree of $L2_1$ ordering, experimental peak intensities and the peak intensities of the fully ordered structure deduced from calculations were compared and ordering parameters were determined. The order parameters S_{L21}, and S_{B2} can be envisaged as a measure of closeness to ideal $L2_1$ and B2 type structures and their deviation from 100% represents the interatomic exchange between the sublattices involved. They can be estimated from the expressions $S_{B2}^2 = I_{200} \cdot I_{400}^{full\ order} / I_{400} \cdot I_{200}^{full\ order}$ and $(S_{L21}\,(3 - S_{B2})\,/2)^2 = I_{111} \cdot I_{220}^{full\ order} / I_{220} \cdot I_{111}^{full\ order}$ where, I_{hkl}, and $I_{hkl}^{full\ order}$ are the experimental diffraction intensities for the (hkl) planes and the reference intensities calculated for the fully ordered alloys, respectively.[19] The calculated values of S_{L21}, and S_{B2} are 88 % and 85 % for x = 0.5, and 94 % and 74 % for x = 0, respectively. This suggests that Co_2TiSi and $Co_2Ti_{0.5}Fe_{0.5}Si$ have mainly ordered $L2_1$ structures with small disorder. However, we found that the $Co_2Ti_{0.75}Fe_{0.25}Si$ has mainly B2-type disordered structure. The XRD patterns show a distinct shift to higher angles indicating that

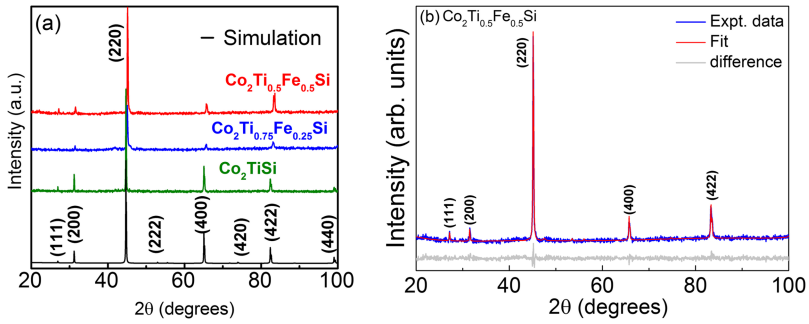

FIG. 1. (a) Powder XRD patterns of $Co_2Ti_{1-x}Fe_xSi$ (x = 0, 0.25, 0.5) alloy prepared by melt spinning and the pattern simulated for $L2_1$ structure of Co_2TiSi compound. (b) experimental data, fit and the difference pattern from the Rietveld analysis of $Co_2Ti_{0.5}Fe_{0.5}Si$ compound. The quality of fit parameters obtained are: R_{exp} = 8.3 %, R_{wp}: 10.7 %, R_p: 8.5 % and R_{Bragg} = 1.7 %.

there is a lattice contraction due to Fe substitution for Ti. In addition, some weak impurity peaks have also been detected in these samples and we carried out the Rietveld analysis of the XRD patterns of all three samples in order to quantify them. The Rietveld analysis shows that the samples with x = 0, x = 0.25 and x = 0.5 respectively contain about 7 wt. %, 13 wt. % and 4 wt. % of $Co_{1-x}Si_x$ type impurity phases. The Rietveld fit along with the experimental data for the $Co_2Ti_{0.5}Fe_{0.5}Si$ is shown in Fig. 1(b) as an example. The lattice constants estimated from the Rietveld analysis are a = 5.729 Å for Co_2TiSi, a = 5.690 Å for $Co_2Ti_{0.75}Fe_{0.25}Si$, and a = 5.677 Å for $Co_2Ti_{0.5}Fe_{0.5}Si$, respectively. These values of a are in good agreement with the calculated lattice constants as discussed below. Moreover, the elemental compositions as determined by EDX analysis are very close (within 4%) to the values estimated from the initial weight of the constituent elements.

Figure 2(a) shows isothermal magnetization curves $M(H)$ of $Co_2Ti_{1-x}Fe_xSi$ (x = 0, 0.25, 0.5) recorded at 5 K with the magnetic field along the length of the ribbons. The $M(H)$ curves have very small coercivities (less than 100 Oe) and the magnetizations saturate at low magnetic fields showing soft magnetic properties. The saturation magnetizations M_s at 5 K are 35 emu/g, 48 emu/g and 87 emu/g for the samples with x = 0, 0.25 and 0.75, respectively, where the M_s shows a systematic increase with the increase in Fe concentration in Co_2TiSi. Further, the $M(H)$ curves of Co_2TiSi and $Co_2Ti_{0.75}Fe_{0.25}$ Si are not fully saturated even at 70 kOe. This may be caused by the presence of a small amount of impurity phase as seen in the Rietveld analysis of XRD data.[21]

Figure 2(b) shows thermomagnetic curves $M(T)$ of $Co_2Ti_{1-x}Fe_xSi$ (x = 0, 0.25, 0.5) alloys measured at 10 kOe, where the magnetization gradually decreases before reaching the Curie temperature. The magnetic transition near the Curie temperature for Co_2TiSi is sharp, whereas that for $Co_2Ti_{0.75}Fe_{0.25}Si$ and $Co_2Ti_{0.5}Fe_{0.5}Si$ is gradual similar to the one observed in some ferrimagnetic compounds.[20] The Curie temperature of Co_2TiSi is 360 K, which increased with Fe substitution

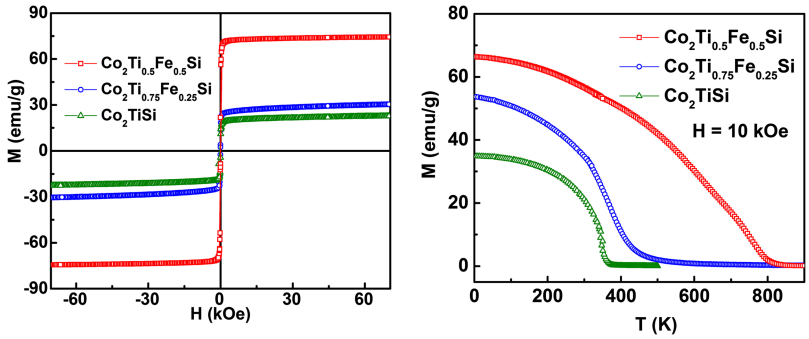

FIG. 2. (a) The magnetic field dependence of magnetization $M(H)$ of $Co_2Ti_{1-x}Fe_xSi$ (x = 0, 0.25, 0.5) at 5 K. (b) The temperature dependence of magnetization of $Co_2Ti_{1-x}Fe_xSi$ (x = 0, 0.25, 0.5) at H = 10 kOe.

reaching 450 K for $Co_2Ti_{0.75}Fe_{0.25}$ Si and about 800 K for $Co_2Ti_{0.5}Fe_{0.5}Si$. We note that the Curie temperature of Co_2FeSi is 1100 K,[21] which is one of the highest values for Heusler compounds. It has been found that the Curie temperature in Co_2-based Heusler compounds varies linearly with their magnetic moments.[22] In other words, for these compounds, higher valence electron concentration corresponds to the higher value of Curie temperature. Since the magnetic moment in our $Co_2Ti_{1-x}Fe_xSi$ samples shows a systematic increase with the increase in Fe concentration, consistent with our first principles calculations, the increase in Curie temperature is expected. Similar increase in the Curie temperature has been observed in Fe doped Co_2CrAl.[13] We may attribute this to the increased positive exchange interaction between the Co and Fe atoms.

The temperature dependence of zero-field resistivity, ρ of $Co_2Ti_{1-x}Fe_xSi$ (x = 0, 0.25, 0.5) ribbons is shown in Fig. 3, where the ρ increases as temperature (T) increases from 5 K to 300 K, showing a

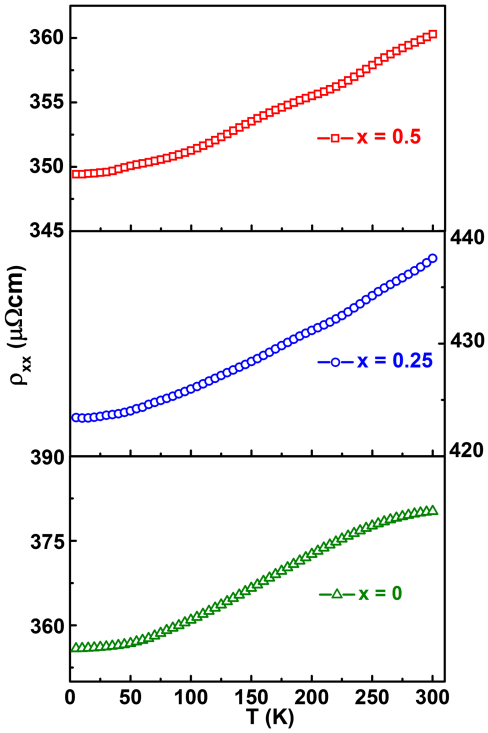

FIG. 3. Longitudinal resistivity ρ_{xx} of $Co_2Ti_{1-x}Fe_xSi$ (x = 0, 0.25, 0.5) as a function of temperature with a zero magnetic field.

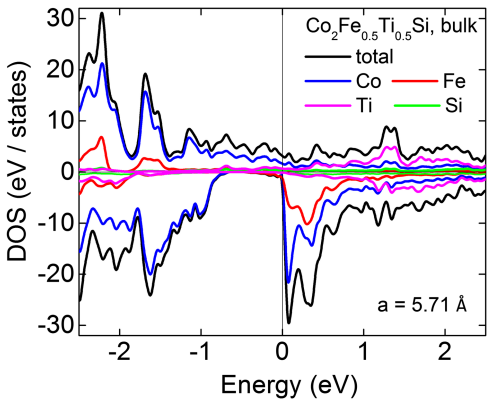

FIG. 4. DOS of the bulk $Co_2Fe_{0.5}Ti_{0.5}Si$ in the ground state. Atomic contributions are color coded as indicated in the figure.

metallic behavior. The residual resistivities (RR) of Co_2TiSi, $Co_2Ti_{0.75}Fe_{0.25}$ Si and $Co_2Ti_{0.5}Fe_{0.5}Si$ are 356 μΩcm, 423 μΩcm and 349 μΩcm, respectively. Interestingly, the sample with B2 type-disorder (x = 0.25) has high RR, showing a direct correlation between the structural disorder and RR of the samples.

B. Computational results

In order to analyze the electronic, structural, and magnetic properties of $Co_2Ti_{1-x}Fe_xSi$ compounds, we performed series of calculations with $Co_{16}Fe_xTi_{(8-x)}Si_8$ supercell varying x between 0 and 7. First, we analyzed how the electronic structure of this material changes as a function of iron concentration. Figure 4 shows the site-projected densities of states (DOS) of $Co_2Ti_{0.5}Fe_{0.5}Si$ (i.e. 50% of Fe concentration) in the ground state, where we see that the Fermi level is pinned at the edge of the minority-spin conduction band, which is composed of Co, and to a lesser degree Fe states. Also, the bottom of the minority-spin band gap is entirely composed of Co states, with no contribution from Fe. The spin-resolved total DOS for $Co_2Ti_{1-x}Fe_xSi$ compound with various Fe concentrations are shown in Fig. 5. These materials show almost half-metallic band structures for low concentration of Fe, i.e., for x < 0.5.

The change in Fe concentration is also found to affect the lattice constant. As shown in the Fig. 6, increasing Fe concentration results in a decrease of the lattice parameter a (black squares), consistent with the XRD results. For smaller Fe concentrations, the decrease in a is small but the change becomes

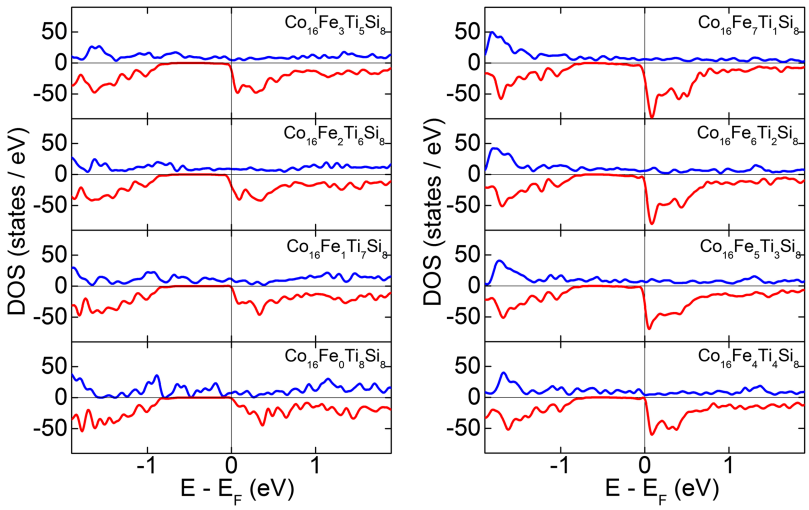

FIG. 5. DOS of $Co_{16}Fe_xTi_{(8-x)}Si_8$ for x ranging from 0 to 7. Positive values (black lines) correspond to majority-, negative values (red lines) to minority-spin states.

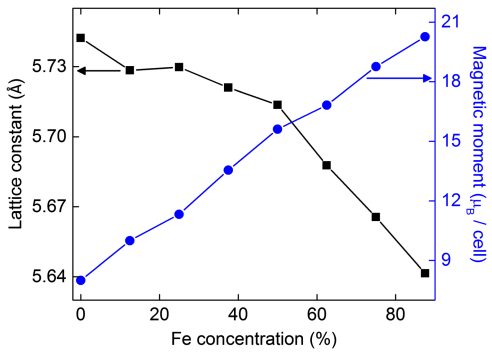

FIG. 6. Lattice constant (black squares) and total magnetic moment (blue circles) of $Co_{16}Fe_xTi_{(8-x)}Si_8$ as a function of Fe concentration.

more prominent for x > 0.5. Our calculations also indicate that increasing Fe concentration results in a steady increase of the total magnetic moment (the atomic contributions are ≈ 1.2 μ_B per Co, and 3.0 μ_B per Fe), as shown on the Fig. 6 (blue circles). This result is in good agreement with our experimental measurements.

IV. CONCLUSIONS

In summary, a combined experimental and theoretical investigation of the structural, magnetic and electronic band properties of $Co_2Ti_{1-x}Fe_xSi$ (x = 0, 0.25, 0.5) Heusler alloys has been carried out. XRD analysis shows that the rapidly quenched $Co_2Ti_{0.5}Fe_{0.5}Si$ crystallized in the cubic $L2_1$ structure whereas $Co_2Ti_{0.75}Fe_{0.25}Si$ and Co_2TiFe_0Si showed various degrees of B2-type disorder. Fe doping increases the saturation magnetization in our samples, and this result is consistent with our calculations. The Curie temperature is enhanced due to Fe substitution from 360 K for Co_2TiSi to about 800 K for $Co_2Ti_{0.5}Fe_{0.5}Si$. The samples are moderately conducting and show metallic electron transport. The first principles calculations show that Fe doped materials are nearly half-metallic for x ≤ 0.5. These interesting results are expected to stimulate further research on the thin films of these materials.

ACKNOWLEDGMENTS

This research is supported by Research/Scholarship Support Fund, SDSU. Research at UNI is supported by the Pre-Tenure Grant from the Office of the Provost and Executive Vice President for Academic Affairs, UNI, as well as from the UNI Faculty Summer Fellowship. Research at UNL is supported by US DOE (DE-FG02-04ER46152, NSF-DMR under Award DMREF: SusChEM 1436385. The work was performed in part in the Nebraska Nanoscale Facility, Nebraska Center for Materials and Nanoscience, which is supported by the National Science Foundation under Award ECCS: 1542182, and the Nebraska Research Initiative.

[1] R. A. de Groot, F. M. Mueller, P. G. v. Engen, and K. H. J. Buschow, Phys. Rev. Lett. **50**(25), 2024–2027 (1983).
[2] M. Jean-Baptiste, J. Phys. D: Appl. Phys. **46**(14), 143001 (2013).
[3] R. J. Soulen, J. M. Byers, M. S. Osofsky, B. Nadgorny, T. Ambrose, S. F. Cheng, P. R. Broussard, C. T. Tanaka, J. Nowak, J. S. Moodera, A. Barry, and J. M. D. Coey, Science **282**(5386), 85–88 (1998).
[4] P. Lukashev, P. Kharel, S. Gilbert, B. Staten, N. Hurley, R. Fuglsby, Y. Huh, S. Valloppilly, W. Zhang, K. Yang, R. Skomski, and D. J. Sellmyer, Appl. Phys. Lett. **108**(14), 141901 (2016).
[5] Y. Jin, P. Kharel, P. Lukashev, S. Valloppilly, B. Staten, J. Herran, I. Tutic, M. Mitrakumar, B. Bhusal, apos, A. Connell, K. Yang, Y. Huh, R. Skomski, and D. J. Sellmyer, J. Appl. Phys. **120**(5), 053903 (2016).
[6] R. Choudhary, P. Kharel, S. R. Valloppilly, Y. Jin, A. O'Connell, Y. Huh, S. Gilbert, A. Kashyap, D. J. Sellmyer, and R. Skomski, AIP Adv. **6**(5), 056304 (2016).
[7] J. Barth, G. H. Fecher, B. Balke, T. Graf, A. Shkabko, A. Weidenkaff, P. Klaer, M. Kallmayer, H.-J. Elmers, H. Yoshikawa, S. Ueda, K. Kobayashi, and C. Felser, Phil. Trans. R. Soc. A **369**(1951), 3588 (2011).
[8] M. Belmeguenai, H. Tuzcuoglu, M. Gabor, T. Petrisor, C. Tiusan, D. Berling, F. Zighem, and S. Mourad Chérif, J. Magn. Magn. Mater **373**, 140–143 (2015).
[9] M. Jourdan, J. Minár, J. Braun, A. Kronenberg, S. Chadov, B. Balke, A. Gloskovskii, M. Kolbe, H. J. Elmers, G. Schönhense, H. Ebert, C. Felser, and M. Kläui, Nat. Commun. **5** (2014).
[10] H. Atsufumi and T. Koki, J. Phys. D: Appl. Phys. **47**(19), 193001 (2014).
[11] Z. Gercsi and K. Hono, J. Phys. Condens. Matter. **19**(32), 326216 (2007).
[12] X.-Q. Chen, R. Podloucky, and P. Rogl, J. Appl. Phys. **100**(11), 113901 (2006).
[13] S. Okamura, R. Goto, S. Sugimoto, N. Tezuka, and K. Inomata, J. Appl. Phys. **96**(11), 6561–6564 (2004).
[14] P. E. Blöchl, Phys. Rev. B **50**(24), 17953–17979 (1994).
[15] G. Kresse and D. Joubert, Phys. Rev. B **59**(3), 1758–1775 (1999).
[16] J. P. Perdew, K. Burke, and M. Ernzerhof, Phys. Rev. Lett. **77**(18), 3865–3868 (1996).
[17] M. Methfessel and A. T. Paxton, Phys. Rev. B **40**(6), 3616–3621 (1989).
[18] MedeA® Version 2.19. MedeA® is a registered trademark of Materials Design, Inc. Angel Fire, New Mexico, USA.
[19] Y. Takamura, R. Nakane, and S. Sugahara, J. Appl. Phys. **105**(7), 07B109 (2009).
[20] M. A. Zagrebin, V. V. Sokolovskiy, and V. D. Buchelnikov, J. Phys. D: Appl. Phys. **49**(35), 355004 (2016).
[21] J. M. Fallon, C. A. Faunce, and P. J. Grundy, J. Phys.: Condens. Matter **12**, 4075 (2000).
[22] S. Wurmehl, G. H. Fecher, H. C. Kandpal, V. Ksenofontov, C. Felser, and H.-J. Lin, Appl. Phys. Lett. **88**, 032503 (2006).